

Models of Defect-Mediated Melting

W. Janke¹

Received May 3, 1990

A survey is given of recent Monte Carlo studies of lattice defect models for melting in three and two dimensions. In two dimensions special emphasis is laid upon a recently proposed model which exhibits a crossover from a single first-order transition to two successive transitions of the Kosterlitz-Thouless type.

1. INTRODUCTION

Many phase transitions can be described in terms of thermally activated topological defects. For the ordinary melting process the usefulness of this approach was emphasized as early as 1952 by Shockley (1952), and for the λ -transition in liquid helium (Kapitza, 1937, 1941) similar ideas were suggested by Onsager (1949) and later employed by Feynman (1955). More recently this idea has been applied to many other physical systems, including liquid crystals (Helfrich, 1978; Nelson and Toner, 1981; Kleinert, 1983*a*), nuclear matter (Kleinert, 1982*a*), and lattice gauge theories (Banks *et al.*, 1977; Wensley and Stack, 1989), to mention a few.

In this paper I would like to report on progress made in the last few years in understanding such defect models for ordinary melting transitions in three and two dimensions. Most quantitative results are obtained from extensive Monte Carlo (MC) simulations of simple lattice models. While in three dimensions a strong first-order melting transition is undisputed, the nature of two-dimensional melting has been very controversial both experimentally and theoretically—and, as we shall see below, also numerically! After a summary of the historical development [for a more detailed exposition and many references, see the comprehensive textbook by Kleinert (1989*a*) and the recent review by Strandburg (1988)], I shall present a new model recently proposed by Kleinert (1988*b*) and its theoretical analysis as well as results of MC simulations (Janke and Kleinert, 1988, 1990). The

¹Institut für Theorie der Elementarteilchen, Freie Universität Berlin, D-1000 Berlin 33, Germany.

new model should be relevant for explaining the systematics observed in recent experimental studies of the two-dimensional melting transition in monolayers consisting of long rodlike molecules (Gay *et al.*, 1988; Larese *et al.*, 1988; Nham and Hess, 1988; Zhang and Migone, 1988, 1989). For a recent review, see Taub (1988).

Structurally, the simplest example for a defect-driven phase transition is the λ -transition in liquid helium, separating the normal and superfluid states. It is well known (Vaks and Larkin, 1965; Bowers and Joyce, 1967) that this transition can be described by a simple lattice model, the (planar) XY model. Since the XY model has served as guideline for all defect models of melting to be discussed below, it is useful to recall first some of its properties.

2. XY MODEL FOR SUPERFLUID HELIUM

The partition function [in Villain's (1975) form] is given by

$$Z_{XY} = \prod_{\mathbf{x}} \left[\int_{-\pi}^{\pi} \frac{d\gamma(\mathbf{x})}{2\pi} \right] \sum_{\{n_i(\mathbf{x})\}} \exp \left[-\left(\frac{\beta}{2}\right) \sum_{\mathbf{x},i} (\nabla_i \gamma - 2\pi n_i)^2 \right] \quad (1)$$

where $\beta \equiv 1/T$ is the (reduced) inverse temperature, $\gamma(\mathbf{x})$ is interpreted as the phase of the superfluid order field, and $\nabla_i \gamma(\mathbf{x}) \equiv \gamma(\mathbf{x} + \mathbf{i}) - \gamma(\mathbf{x})$ are the lattice gradients in the \mathbf{i} direction of a D -dimensional simple cubic (sc) lattice. The integer variables n_i are the lattice analogs of plastic deformations (jumps of γ by 2π) forming "Volterra surfaces" whose boundaries are the defects. Since the surfaces themselves are physically irrelevant, they may be interpreted as gauge fields of defects (Kleinert, 1982*d*, 1983*f*, 1988*a*).

D = 3 Dimensions. In three dimensions, the defects described by (1) are linelike objects, related to $n_k(\mathbf{x})$ by $l_i(\mathbf{x}) = \varepsilon_{ijk} \nabla_j n_k(\mathbf{x} + \mathbf{i})$. In helium they are interpreted as thermally activated vortex lines, destroying the superfluid state along their cores. Their statistical mechanics is governed by the partition function

$$Z_{XY} \propto \sum_{\{l_i\}} \left[\prod_{\mathbf{x}} \delta_{\nabla_i l_i, 0} \right] \exp \left[-4\pi^2 \beta \frac{1}{2} \sum_{\mathbf{x}, \mathbf{x}'} l_i(\mathbf{x}) v_C^{3D}(\mathbf{x} - \mathbf{x}') l_i(\mathbf{x}') \right] \quad (2)$$

which can be derived from (1) by a duality transformation (Savit, 1980). The interaction of vortex lines is of the long-range Coulomb type (modified by lattice effects)

$$v_C^{3D}(\mathbf{x}) \equiv \int_{-\pi}^{\pi} \frac{d^3 k}{(2\pi)^3} \frac{\exp(i\mathbf{k}\mathbf{x})}{2 \sum_{i=1}^3 (1 - \cos k_i)} \approx \frac{4\pi}{|\mathbf{x}|} \quad (|\mathbf{x}| \gg 1) \quad (3)$$

and the constraints $\bar{\nabla}_i l_i(\mathbf{x}) \equiv l_i(\mathbf{x}) - l_i(\mathbf{x} - \mathbf{i}) = 0$ ensure that the lines form closed networks, i.e., loops. Two typical loop configurations, constructed from MC simulations of (1), are shown in Figure 1 (Janke, 1985). From

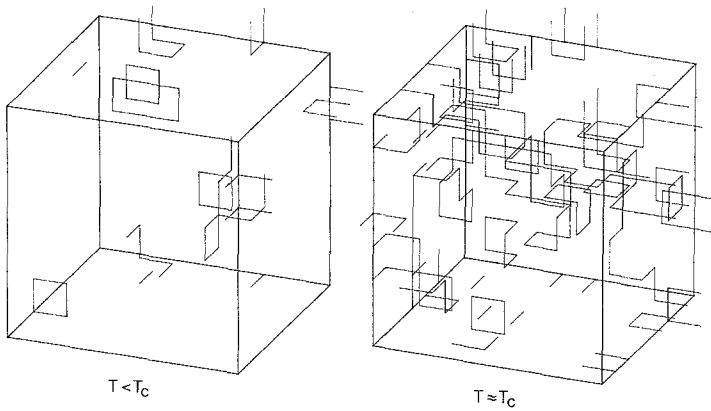


Fig. 1. Typical vortex-loop configurations of the three-dimensional XY model.

such MC simulations it is known that the model undergoes a continuous phase transition at $\beta_c \approx 0.33$ (Dasgupta and Halperin, 1981; Janke, 1985; Janke and Kleinert, 1986a). The critical exponent α , associated with the singularity of the specific heat at β_c , is found to be slightly negative, in agreement with experiments on liquid helium by Mueller *et al.* (1976) ($\alpha = -0.026 \pm 0.004$) and Lipa and Chui (1983) ($\alpha = -0.0127 \pm 0.0026$). Unfortunately, working directly with the defect picture (2), it is very hard to reproduce these results analytically (Byckling, 1965; Popov, 1973; Wiegel, 1973, 1975, 1986; Gupte and Shenoy, 1986; Williams, 1987; Shenoy, 1989; Lund *et al.*, 1990).

On the other hand, it is very easy (Feynman, 1955, p. 52) to convince oneself that linelike defects are in principle able to drive a phase transition. The point is that, although the activation energy per line element, ϵ , is usually very large (corresponding, e.g., for crystalline defects to $\sim 10,000$ K), at sufficiently high temperatures this energy can always be overcompensated by the large entropy of linelike structures. In order to see this, consider a line with n elements on an sc lattice. Suppose we neglect all long-range interactions and short-range constraints of steric origin. Then each line element has $2D$ possible orientations, and the whole line contributes to the partition function

$$(2D)^n e^{-\beta(n\epsilon)}$$

Summing over all line lengths, we find

$$Z \propto \sum_n e^{-n[\beta\epsilon - \ln(2D)]}$$

This diverges for $\beta < \ln(2D)/\epsilon$ or

$$T > T_c = \epsilon/\ln(2D)$$

signaling the proliferation of defect lines. Certainly, this simple energy-entropy balance is only a very rough estimate, but it does show the basic origin for defect-line-mediated phase transitions.

D = 2 Dimensions. In two dimensions, the partition function (1) describes superfluid films and the vortex lines $l_i(\mathbf{x})$ degenerate to vortex points, $m(\mathbf{x}) = \varepsilon_{ij} \nabla_i n_j(\mathbf{x})$. The two-dimensional analog of (2),

$$Z_{XY} \propto \sum_{\{m\}} \exp \left[-4\pi^2 \beta \frac{1}{2} \sum_{\mathbf{x}, \mathbf{x}'} m(\mathbf{x}) v_C^{2D}(\mathbf{x} - \mathbf{x}') m(\mathbf{x}') \right] \quad (4)$$

can be interpreted as a Coulomb gas with charges $m(\mathbf{x})$ interacting via a logarithmic potential

$$v_C^{2D}(\mathbf{x}) \equiv \int_{-\pi}^{\pi} \frac{d^2 k}{(2\pi)^2} \frac{\exp(i\mathbf{k}\mathbf{x}) - 1}{2 \sum_{i=1}^2 (1 - \cos k_i)} \approx -\frac{1}{2\pi} \ln|\mathbf{x}| \quad (|\mathbf{x}| \gg 1) \quad (5)$$

Another useful representation, equivalent to (1) and (4), is the so-called discrete Gaussian (DG) model,

$$Z_{XY} \propto Z_{\text{DG}} = \sum_{\{h\}} \exp \left[-\beta^{\text{DG}} \sum_{\mathbf{x}} (\nabla_i h)^2 \right] \quad (6)$$

with $\beta^{\text{DG}} = 1/2\beta$ and integer-valued height variables $h(\mathbf{x})$, which was originally invented for describing surface roughening phenomena (Burton *et al.*, 1951).

The two-dimensional system undergoes a very peculiar phase transition which can be described by renormalization group arguments applied to the defect representation (4). According to Kosterlitz and Thouless (1973, 1978) (KT) [see also Berezinskii (1970, 1971), Kosterlitz (1974), and the recent review by Minnhagen (1987)], the transition is caused by the dissociation of vortex-antivortex pairs which are tightly bound at low temperatures. Their analysis shows that, below the critical temperature ($\beta > \beta_c$), the physics is governed by massless phononlike excitations, leading to an infinite correlation length in the system. The dilute gas of bound defects manifests itself only in a renormalization of the temperature, i.e., $\beta \rightarrow \beta^{\text{R}}$. This picture breaks down at the critical point β_c , where β^{R} approaches the universal value

$$\beta_c^{\text{R}} \equiv \beta^{\text{R}}(\beta_c) = 2/\pi \quad (7)$$

For higher temperatures ($\beta < \beta_c$), the correlations are massive and the correlation length is finite. The renormalized coupling β^{R} can be determined by measuring correlation functions in the massless phase. For instance, in the roughening representation (6) one can show (Shugard *et al.*, 1978) that at long distances

$$\frac{1}{2} \langle [h(\mathbf{x}) - h(\mathbf{x}')]^2 \rangle = -\beta^{\text{R}}(\beta) v_C^{2D}(\mathbf{x} - \mathbf{x}') \quad (8)$$

with v_C^{2D} given in (5). The critical point β_c can then be determined by

varying β until β^R hits $2/\pi$. A recent MC study (Janke and Kleinert, 1988, 1990) along these lines gave $\beta_c = 0.739 \pm 0.011$ or $\beta_c^{DG} = 0.677 \pm 0.010$. Notice that in a KT transition the smooth peak of the specific heat does *not* locate the transition point, but is displaced by $\sim 20\%$ to higher (lower) temperatures T (T^{DG}) [e.g., $\beta_{\text{peak}}^{DG} = 0.861 \pm 0.005$ (Janke and Kleinert, 1988, 1990)].

3. FIRST-GRADIENT DEFECT MODEL FOR MELTING

The starting point is the well-known energy of classical elasticity in the continuum (\cong long-wavelength) approximation,

$$E_C^{(1)} = \int d^D x \left[\mu \left(\sum_{i \neq j} u_{ij}^2 + \xi \sum_i u_{ii}^2 \right) + \frac{\lambda}{2} \left(\sum_i u_{ii} \right)^2 \right] \quad (9)$$

where $u_{ij} \equiv (\partial_i u_j + \partial_j u_i)/2$ is the total strain, u_i are the displacements, and $\xi = (c_{11} - c_{12})/2c_{44}$, $\lambda = c_{12}$, $\mu = c_{44}$ are elastic constants. To account for crystalline defects, $E_C^{(1)}$ is then extended in analogy to (1) by plastic distortions, replacing $\partial_i u_j$ by $\partial_i u_j^{el} = \partial_i u_j - \beta_{ij}^P$, and u_{ij} by $u_{ij}^{el} = u_{ij} - u_{ij}^P$, with $u_{ij}^P = (\beta_{ij}^P + \beta_{ji}^P)/2$. Finally, to obtain a lattice model similar to (1), differentials are replaced by finite differences, $\partial_i u_j \rightarrow \nabla_i u_j/a$ (a = lattice constant), and plastic distortions by integer-valued ‘‘plastic jumps,’’ $\beta_{ij}^P \rightarrow n_{ij}$. After rescaling u_i to $\gamma_i = 2\pi u_i/a$ and setting $\beta \equiv \mu a^D/(2\pi)^2 k_B T$, the ensuing partition function for defect melting reads (Kleinert, 1982c)

$$\begin{aligned} Z^{(1)} &= \prod_{\mathbf{x}, i} \left[\int_{-\pi}^{\pi} d\gamma_i(\mathbf{x}) \right] \sum_{\{n_{ij}, i \neq j\}} \exp(-\beta E^{(1)}) \\ E^{(1)} &= \sum_{\mathbf{x}} \left[\frac{1}{2} \sum_{i < j} (\nabla_i \gamma_j + \nabla_j \gamma_i - 4\pi n_{ij}^s)^2 + \xi \sum_i (\nabla_i \gamma_i - 2\pi n_{ii}^s)^2 \right. \\ &\quad \left. + \frac{\lambda}{2\mu} \left\{ \sum_i [\nabla_i \gamma_i(\mathbf{x} - \mathbf{i}) - 2\pi n_{ii}^s(\mathbf{x} - \mathbf{i})] \right\}^2 \right] \quad (10) \end{aligned}$$

where $n_{ij}^s \equiv (n_{ij} + n_{ji})/2$. Notice that n_{ij}^s is *half-integer* for $i \neq j$ and that the antisymmetric combination $n_{ij}^a \equiv (n_{ij} - n_{ji})/2$ does not enter in (10). This degeneracy will be lifted in the second-gradient model discussed in Section 4.

D = 3 Dimensions. By generalizing the duality transformation from (1) to (2), it has been verified (Kleinert, 1983c,d) that in three dimensions the defect loops described by (10) interact via the known long-range forces (Blin’s law). From this defect representation, an excellent low-temperature approximation can be obtained (Janke and Kleinert, 1986b) by taking into account only those defect configurations with lowest energy (see Figure 2). In the opposite limit of high temperatures, a similar analysis is possible in the dual stress representation of (10) (Kleinert, 1983c,d), which consists also of an ensemble of closed lines, but with no long-range interactions.

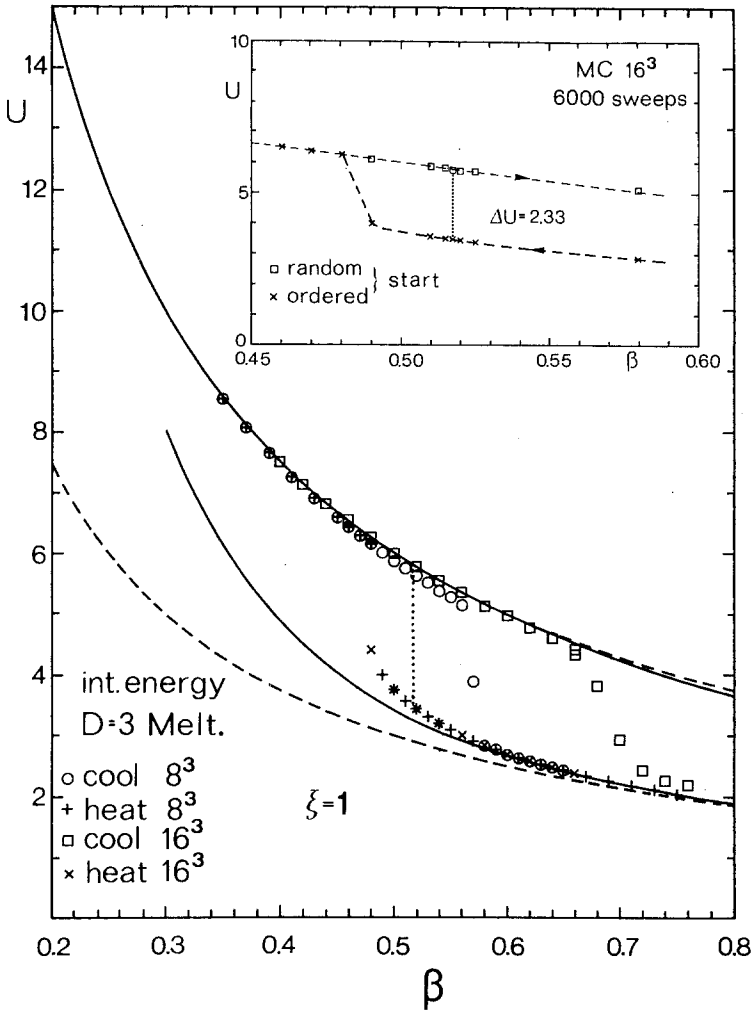


Fig. 2. Internal energy of the three-dimensional defect melting model (10). The solid lines show low- and high-temperature expansions calculated respectively from the defect- and stress-loop representations of the model. The inset shows a blowup of the transition region.

By comparing the free energies of both approximations, a strong first-order transition is predicted (Janke and Kleinert, 1986*b*) around $\beta_m \approx 0.52$. To test this theoretical prediction, we have performed MC simulations of (10) on sc lattices with periodic boundary conditions (Janke and Kleinert, 1986*b*). [For a related MC study, see also Jacobs and Kleinert (1984).] The resulting internal energy for $\xi = 1, \lambda = 0$ displayed in Figure 2 shows indeed

a pronounced hysteresis, typical for a first-order transition. To locate the transition point more precisely, we have applied the so-called mixed-start technique, which is explained schematically in Figure 3a and illustrated by our data in Figure 3b. We conclude that the transition takes place at $\beta_m = 0.5175 \pm 0.0025$ with latent heat $\Delta U \approx 2.33$ and transition entropy $\Delta S = \beta_m \Delta U \approx 1.21$. Notice that both transition point (corresponding to a Lindemann number $L \approx 112$) and transition entropy have the magnitude observed in many materials (see, e.g., Ubbelohde, 1978, Table 3.7). Also, the variation with the anisotropy parameter ξ was found in good agreement with experimental results (Ubbelohde, 1978).

D = 2 Dimensions. While in three dimensions a first-order melting transition is undisputed, the nature of two-dimensional melting has been very controversial (Strandburg, 1988). Generalizing the work of Kosterlitz and Thouless (1973, 1978) (KT) on superfluid films, Halperin and Nelson (1978) [see also Nelson (1979) and Nelson and Halperin (1979)] and Young (1979) (HNY) suggested that melting in two dimensions should proceed via two successive pair unbinding transitions of the KT type. According to KTHNY, as temperature increases, in the first transition pairs of dislocations should dissociate, while in the second, dislocations are supposed to split into pairs of disclinations. Alternative theories predict a single first-order transition caused by the proliferation of chains of dislocation-antidislocation pairs (Kleinert, 1983*b,e*), or by related grain boundary mechanisms (Chui, 1982, 1983).

Both theories have been applied (Nelson, 1982; Kleinert, 1983*b,e*) explicitly to the partition function (10), thus predicting different types of phase transitions for this model in $D = 2$ dimensions. In order to decide which alternative is correct, several MC simulations have been performed, which, however, also yielded conflicting results. In our MC simulations of (10) on square lattices (Janke and Kleinert, 1984, 1986*c*) we found clear evidence for a single first-order transition.² Around the transition point, $\beta_m = 0.815 \pm 0.005$ ($\xi = 1, \lambda = 0$), we observed long-lived metastable states (see Figure 4) and a corresponding hysteresis in the internal energy (see Figure 5) (Janke and Kleinert, 1986*c*). The transition is, however, much weaker than in three dimensions, as can be inferred from the estimate for the transition entropy, $\Delta S \approx 0.24$.

By a standard duality transformation, the partition function (10) for $\xi = 1$ can be shown to be equivalent to the so-called Laplacian roughening

²In the first study (Janke and Kleinert, 1984), the periodic Gaussians in (10) were replaced by exponentials of cosines. This simplifies some considerations (see also Ami and Kleinert, 1984). The relation between the two representations is discussed in detail by Janke and Kleinert (1986*a,c*).

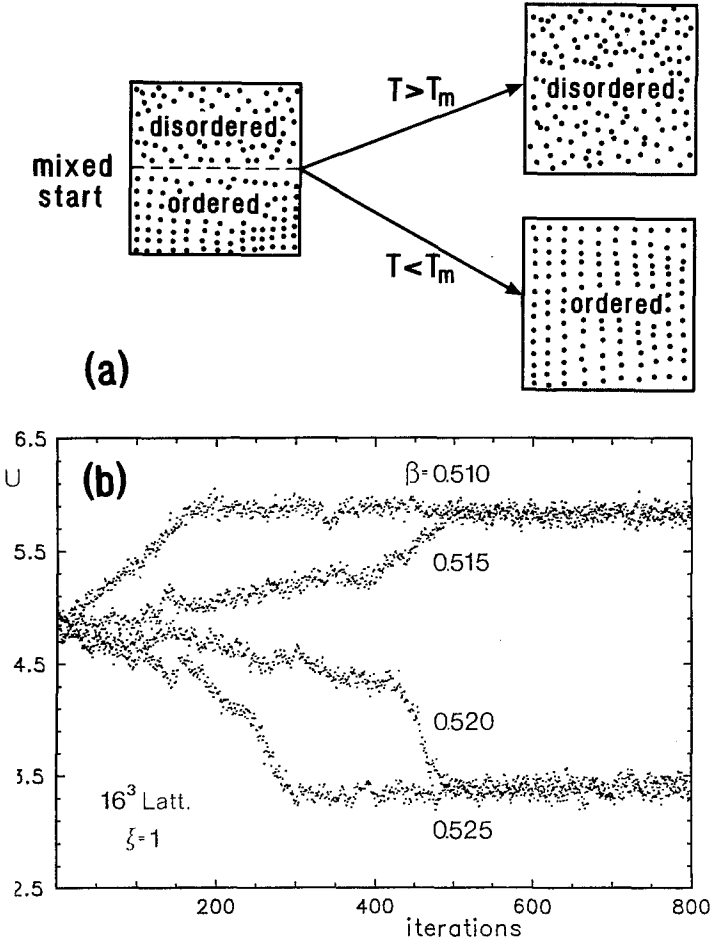


Fig. 3. (a) The mixed-start technique for locating first-order transitions. Starting with a mixed configuration, after a few MC sweeps the system equilibrates to the ordered or disordered state, depending on the temperature. Only for $T = T_m$ do the two phases coexist. (b) Application of the mixed-start technique to the three-dimensional defect melting model (10), determining $\beta_m \equiv 1/T_m = 0.5175 \pm 0.0025$.

(LR) model (Nelson, 1982),

$$Z^{(1)} \propto Z_{LR} = \sum_{\{h\}} \exp \left[-(\beta^{LR}/2) \sum_{\mathbf{x}} (\bar{\nabla} \nabla h)^2 \right] \quad (11)$$

where $\beta^{LR} = 1/2\beta(1 + \nu)$ with $\nu = \lambda/(\lambda + 2\mu)$ being Poisson's ratio. The $h(\mathbf{x})$ are integer-valued height variables, and the lattice Laplacian is given by $\bar{\nabla} \nabla h(\mathbf{x}) \equiv \sum_{\mathbf{i}} [h(\mathbf{x} + \mathbf{i}) - h(\mathbf{x})]$, with \mathbf{i} pointing to the 4 nearest neighbors

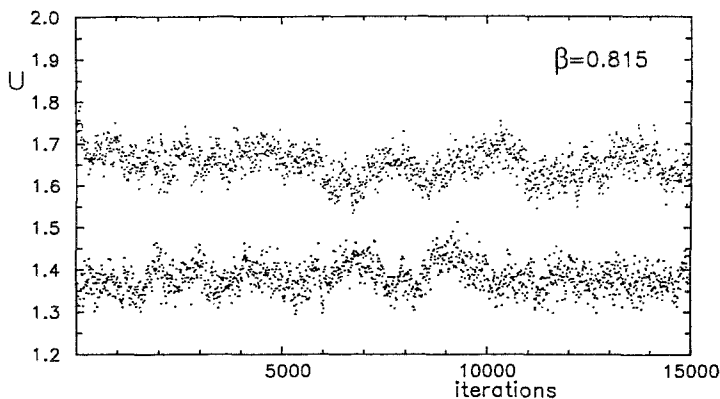


Fig. 4. Stability runs for the two-dimensional defect melting model (10) on a 60×60 square lattice at the inverse transition temperature $\beta_m = 0.815$.

of the site \mathbf{x} . While we were able to confirm the first-order transition at $\beta_m^{\text{LR}} = 1/(2 \times 0.815) = 0.613$ by independent simulations of the partition function (11) (Janke and Kleinert, 1985), Bruce (1985) has claimed evidence for a sequence of two KT transitions as suggested by the KTHNY mechanism. In another study of this model on a triangular lattice, Strandburg *et al.* (1983) (see also Strandburg, 1986) reached the same conclusion from an analysis of correlation functions on 32×32 lattices. {On a triangular lattice the Laplacian in (11) is defined as $\bar{\nabla} \nabla h(\mathbf{x}) \equiv \frac{2}{3} \sum_{\mathbf{i}} [h(\mathbf{x} + \mathbf{i}) - h(\mathbf{x})]$, with \mathbf{i} pointing to the 6 nearest neighbors.}

For the square lattice these results are clearly contradictory. For the triangular lattice, on the other hand, it was conceivable that the different lattice geometry is responsible for a different type of phase transition. In order to clarify this situation, we have recently undertaken high-statistics simulations (with up to 12 million sweeps per data point!) of the LR model (11) on triangular lattices with up to 72×72 sites, thereby focusing on thermodynamic quantities such as energy and specific heat (Janke and Toussaint, 1986; Janke and Kleinert, 1989). Our main result is the strong finite-size dependence of the narrow specific-heat peak shown in Figure 6, which definitely favors a single first-order transition (at $\beta_m^{\text{LR}} = 0.5385 \pm 0.0010$) (Janke and Kleinert, 1989). As mentioned above, the alternative, a sequence of two KT transitions, would be signaled by two *smooth* peaks, which, moreover, should be only weakly lattice-size dependent. Since this is obviously not the case, we concluded that of the two alternatives, a single first-order transition is much more likely. More quantitatively, this conclusion is tested in the inset of Figure 6, which shows a finite-size scaling plot, presuming a first-order transition (in which the peak height, for large

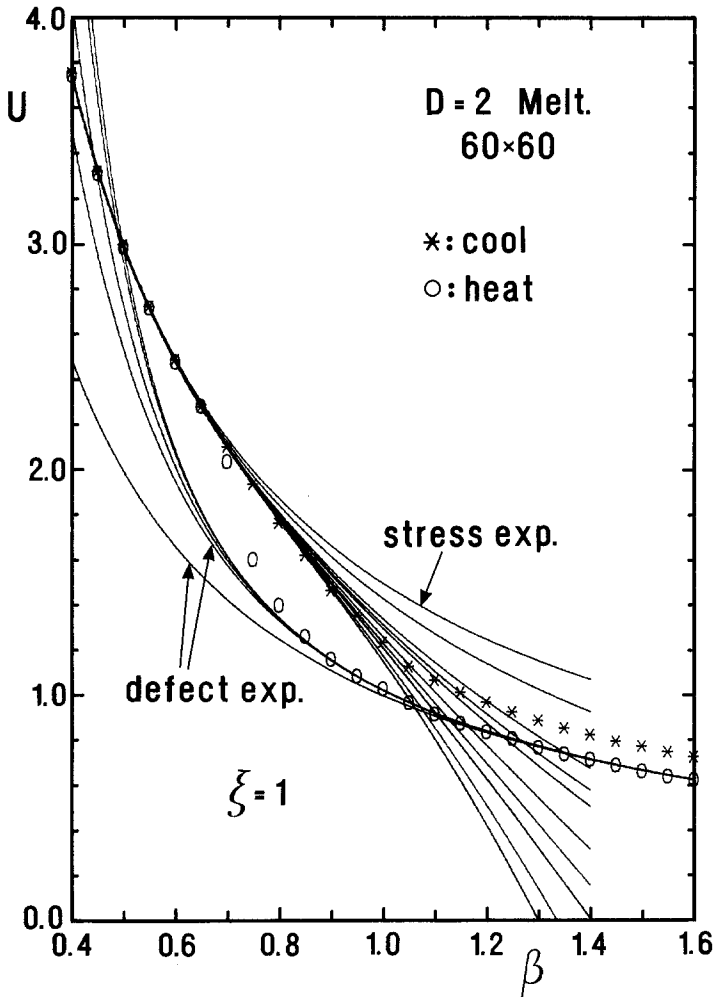


Fig. 5. Internal energy of the two-dimensional defect melting model (10) on a square lattice. The solid lines show low- and high-temperature expansions calculated respectively from the defect and stress representations of the model.

L , scales with lattice volume $V = L^2$, and the peak width with $1/V$). The observed clustering of our data around a common curve clearly confirms this ansatz. In Figure 7 the asymptotic linear scaling of the peak height with V is demonstrated more directly, and using the relation “slope” = $(\Delta S)^2/4$, we can estimate the transition entropy, $\Delta S \approx 0.08$. From these extensive MC simulations we thus conclude that two-dimensional melting,

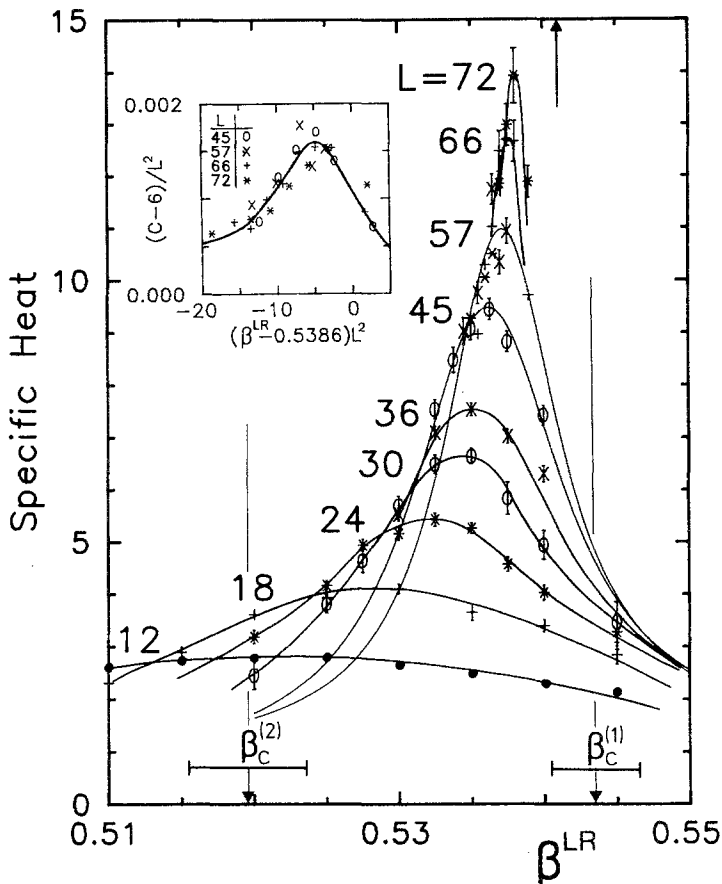


Fig. 6. Finite-size scaling behavior of the specific heat near the phase transition of the Laplacian roughening model (11) on $L \times L$ triangular lattices. $\beta_c^{(1)}$ and $\beta_c^{(2)}$ are the KT transition points reported by Strandburg *et al.* (1983), and the arrow at the top line shows their estimate for the location of the peak maximum on a 32×32 lattice. The inset shows a finite-size scaling plot of our data, presuming a first-order transition.

on the basis of the first-gradient model (10), shows a single, weak first-order transition. (At least if we exclude a completely novel type of phase transition not covered by either of the available theories.)

4. SECOND-GRADIENT DEFECT MODEL FOR MELTING

In the last decade, numerous experiments on two-dimensional melting have been reported in the literature (Strandburg, 1988). Also here conflicting results have been claimed, and many technical problems had to be solved

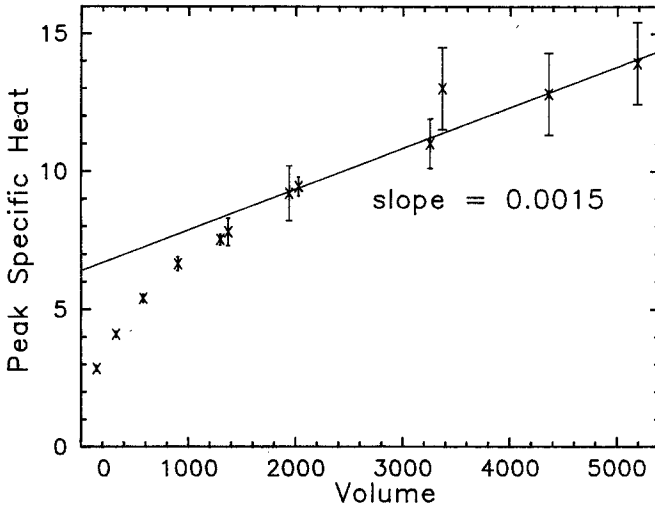


Fig. 7. Maxima of the specific heat peaks shown in Figure 6 versus the lattice volume $V = L^2$. The slope of the linear fit, characteristic for a first-order transition, is related to the transition entropy.

(influence of the substrate, usually graphite or argon; dependence on the coverage, i.e., average “thickness” of the layer; etc.). Only recently has a systematic emerged according to which *atomic* layers show a single, sharp transition, while melting of layers of *rodlike molecules* is a smooth process. (Gay *et al.*, 1988; Larese *et al.*, 1988; Nham and Hess, 1988; Zhang and Migone, 1988, 1989). For a recent review, see Taub (1988).

Motivated by this observation, Kleinert (1988*b*) has recently generalized the model (10) by taking into account also higher gradients of the displacements, $\partial_i \partial_j u_k$. These appear quite naturally in the variations of local rotations, $\partial_i \omega_j$, where

$$\omega_j(\mathbf{x}) = \frac{1}{2} \varepsilon_{jkl} \partial_k u_l(\mathbf{x}) \quad (D=3) \quad (12)$$

is the local rotation field. If also rotational plastic deformations, $\partial_i \omega_j^P = \frac{1}{2} \partial_i \varepsilon_{jkl} \beta_{kl}^P + \Phi_{ij}^P$, are taken into account, the second-gradient energy reads in the continuum approximation

$$E_C^{(2)} = 2\mu l^2 \int d^3x (\partial_i \omega_j - \partial_i \omega_j^P)^2 \quad (13)$$

where the parameter l is called the length scale of rotational stiffness, being small (or zero) for atomic crystals, but large for crystals formed by long rodlike molecules. For simple systems, the value of l has been estimated analytically (Kleinert, 1989*b*) by studying (transverse) dispersion relations, $\omega_T^2 = c^2 k^2 (1 + l^2 k^2 + \dots)$.

Here we shall not go into the details (Kleinert, 1989a) of the three-dimensional generalization of (10) based on both energies $E_C^{(1)}$ and $E_C^{(2)}$, since in three dimensions no qualitative modifications are expected. Rather, we proceed immediately to the more crucial case of two dimensions where the second-gradient energy plays a distinguishing role.

D = 2 Dimensions. In two dimensions, the local rotation field degenerates to the $j = 3$ component of ω_j in (12) ($\varepsilon_{3jk} \equiv \varepsilon_{jk}$),

$$\omega \equiv \omega_3 = \frac{1}{2}\varepsilon_{jk}\partial_j u_k = \frac{1}{2}(\partial_1 u_2 - \partial_2 u_1) \quad (D = 2) \quad (14)$$

and $\partial_i \omega^P$ becomes $\frac{1}{2}\partial_i \varepsilon_{jk} \beta_{jk}^P + \kappa_i^P$. Proceeding as before, i.e., replacing differentials by differences and plastic deformations by integer-valued jumps, $\beta_{ij}^P \rightarrow n_{ij}$, $a\kappa_i^P \rightarrow m_i$, the lattice version of (13) becomes (Kleinert, 1988b)

$$E^{(2)} = 2(l/a)^2 \sum_{\mathbf{x}, i} [\nabla_i \omega - 2\pi(m_i + \nabla_i n_{12}^a)]^2 \quad (15)$$

where $n_{12}^a \equiv (n_{12} - n_{21})/2$ is the antisymmetric combination of n_{ij} . With the combined energy $E = E^{(1)} + E^{(2)}$, the degeneracy in (10) is thus removed and the generalized partition function for second-gradient defect melting can be written as

$$Z^{(2)} = \prod_{\mathbf{x}, i} \left[\int_{-\pi}^{\pi} d\gamma_i(\mathbf{x}) \right] \sum_{\{n_{ij}\}} \sum_{\{m_i\}} \exp[-\beta(E^{(1)} + E^{(2)})] \quad (16)$$

By going through standard duality transformations (Kleinert, 1988b; Janke and Kleinert, 1988, 1990), we can rewrite $Z^{(2)}$ in terms of defect fields for dislocations and disclinations, similarly to the vortex representation (4). While this has the most direct physical interpretation, for MC simulations, the dual representation in terms of integer-valued stress gauge fields h , A is more convenient. This takes the form of a roughening model [similar to (6) and (11)],

$$Z^{(2)} \propto \sum_{\{A_i, h\}} \exp \left[-\frac{1}{\beta} \sum_{\mathbf{x}} \left\{ \frac{1}{4} \left[\frac{1}{1+\nu} (\bar{\nabla}_i A_j)^2 - \frac{1}{2} \frac{1-\nu}{1+\nu} (\bar{\nabla}_i A_i)^2 \right] + \frac{1}{8(l/a)^2} (\bar{\nabla}_i h - \varepsilon_{ij} A_j)^2 \right\} \right] \quad (17)$$

From now on we shall measure lengths in units of the lattice spacing so that $a \equiv 1$.

Let us briefly discuss three limiting cases of $Z^{(2)}$ in (17):

(a) In the limit $l \rightarrow 0$, the last term enforces $A_i = -\varepsilon_{ij} \bar{\nabla}_j h$ and $Z^{(2)}$ reduces to the LR model (11) with $\beta_{LR} = 1/2\beta(1 + \nu)$, as it should by construction. Using the previously determined value for β_m^{LR} on a square lattice, we hence expect a first-order transition at $T_m \equiv 1/\beta_m \approx 2.45(1 + \nu)/2$.

(b) In the limit $l \rightarrow \infty$, $\beta \rightarrow 0$ with βl^2 fixed, the fields A_i are squeezed to zero and (17) becomes effectively the DG model (6) with $\beta^{\text{DG}} = 1/8\beta l^2$. Inserting the values quoted in Section 2, this implies for large l a line of KT transitions given by $T_c^{(2)}(l) = 8l^2\beta_c^{\text{DG}} \approx 5.42l^2$, with associated specific heat peaks at $T_{\text{peak}}^{(2)}(l) = 8l^2\beta_{\text{peak}}^{\text{DG}} \approx 6.89l^2$.

(c) Finally, for $l \rightarrow \infty$ with $\beta \approx 1$, the field h can be treated approximately as continuous, and performing the Gaussian integrals, we end up with

$$Z^{(2)} \rightarrow \sum_{\{A_i\}} \exp \left[-\frac{1}{\beta} \sum_x \left\{ \frac{1}{4} \left[\frac{1}{1+\nu} (\bar{\nabla}_i A_j)^2 - \frac{1}{2} \frac{1-\nu}{1+\nu} (\bar{\nabla}_i A_i)^2 \right] + \frac{1}{8l^2} A_i \frac{1}{-\bar{\nabla}^2} (-\nabla_i \bar{\nabla}_j) A_j + \dots \right\} \right] \tag{18}$$

In Kleinert (1988b) and Janke and Kleinert (1988, 1990) it is shown that the *qualitative* behavior of (18) does not depend on ν . Here we shall discuss only the simplest case $\nu = 1$, corresponding to $\lambda = \infty$, i.e., incompressible material. At *infinite* l , the last term vanishes and we have then two decoupled DG models, implying KT transitions at $T_c^{(1)} = 8\beta_c^{\text{DG}} \approx 5.42$ with specific heat peaks at $T_{\text{peak}}^{(1)} = 8\beta_{\text{peak}}^{\text{DG}} \approx 6.89$. For large but *finite* l , the specific heat receives only small corrections. The transition temperatures, however, are lower by a factor of about 2 due to the long-range interactions generated by the inverse difference operator in the last term of (18) (Kleinert, 1988b; Janke and Kleinert, 1988, 1990).

In order to map out the full phase diagram in the l^2 - T ($=1/\beta$) plane presented in Figure 8, we have performed extensive MC simulations in the roughening representation (17) on square lattices with periodic boundary conditions (Janke and Kleinert, 1988, 1990). We have always put $\nu = 1$, for simplicity. Because of the expected KT transitions for large l , we have measured both specific heats, for a rough overview, and correlation functions, for a precise determination of the transition points.

Our specific heat curves on a 16×16 square lattice are shown in Figure 9. For small l we see a single sharp peak consistent with a first-order transition. For $l^2 \approx 1.2$, it splits into two separated peaks which, with increasing l , both become very smooth, as expected for KT transitions. Indeed, their location and shape are in good agreement with the theoretical predictions based on the effective DG model representations. Furthermore, we have checked that for $l^2 > 2$, the peaks are almost lattice-size independent as required for KT transitions.

Our correlation functions are defined by

$$c^h(x-x') \equiv \frac{1}{2} L \langle [\bar{h}(x) - \bar{h}(x')]^2 \rangle$$

$$c^{A_i}(x-x') \equiv \frac{1}{2} L \langle [\bar{A}_i(x) - \bar{A}_i(x')]^2 \rangle, \quad i = 1, 2 \tag{19}$$

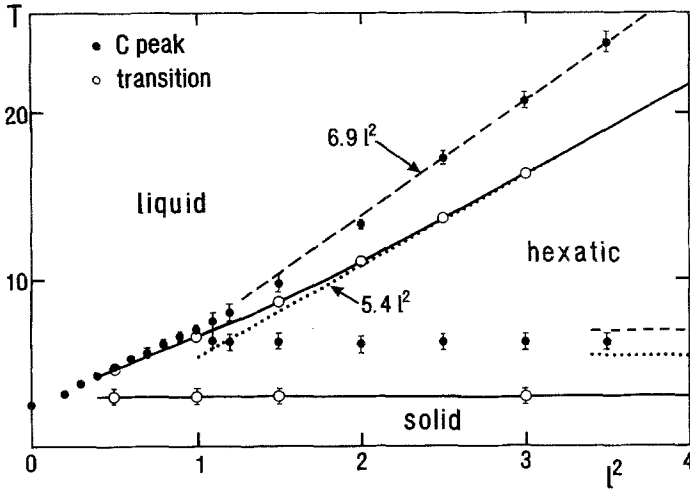


Fig. 8. Phase diagram of the two-dimensional second-gradient defect model for $\nu = 1$. Here $T \equiv 1/\beta$ is the (reduced) temperature and l is the length scale of rotational stiffness (in lattice units). The transition points are determined from measurements of correlation functions (see Figure 10). The dashed and dotted straight lines are calculated from the effective DG model representations for large l . The solid curves interpolating the MC data are only to guide the eye.

where $\langle \dots \rangle$ are thermal averages and the bars denote a configuration average along one column, e.g., $\bar{h}(x) = L^{-1} \sum_{y=1}^L h(x, y)$. In momentum space these averages are equivalent to projections onto the k_x axis, leading to one-dimensional Fourier representations which, in the free-field case, can be evaluated analytically even on finite lattices.

In the low-temperature “solid”³ phase for large l (and $\nu = 1$), the expected behaviors of these correlation functions at long range are [compare equation (8)]

$$\begin{aligned}
 c^h(x) &= -4\beta^R [c_4(x) + l^2 c_2^{(0)}(x)] \\
 c^{A_1}(x) &= -4\beta^R c_2^{(1/l)}(x) \\
 c^{A_2}(x) &= -4\beta^R c_2^{(0)}(x)
 \end{aligned}
 \tag{20}$$

with $c_2^{(m)}$ and c_4 given by $[k = (2\pi/L)n]$

$$\begin{aligned}
 c_2^{(m)}(x) &= \frac{1}{L} \sum_{n=1}^{L-1} \frac{e^{ikx} - 1}{2(1 - \cos k) + m^2} \\
 c_4(x) &= \frac{1}{L} \sum_{n=1}^{L-1} \frac{e^{ikx} - 1}{[2(1 - \cos k)]^2}
 \end{aligned}
 \tag{21}$$

³We have tentatively identified the three phases according to their defect structures, although we have not yet performed any detailed structural investigations to confirm these phase properties.

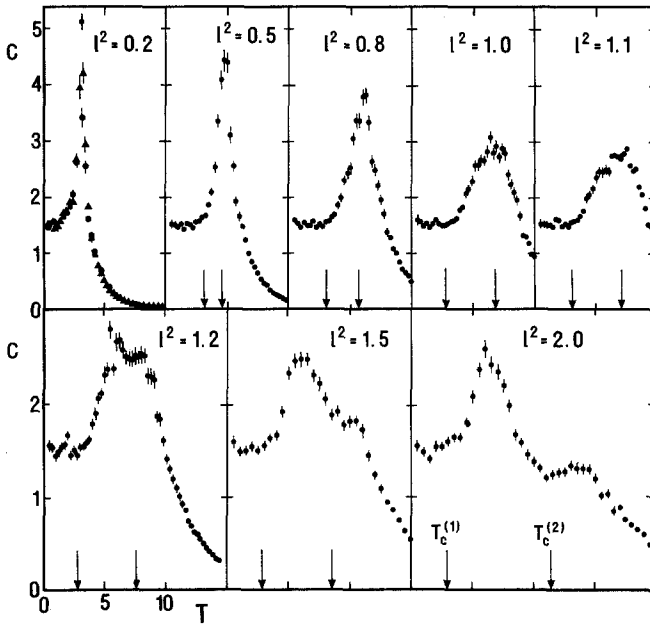


Fig. 9. Specific heat of the two-dimensional second-gradient defect model on a 16×16 square lattice for increasing length scale of rotational stiffness l . The arrows indicate the transition points, which, for $l^2 > 1$, are clearly displaced to lower temperatures compared with the peaks. The MC data are averages over 5000 configurations, after discarding 1000 configurations for thermalization.

At the phase transition to the intermediate “hexatic” phase (see footnote 3), the standard KT argument predicts

$$\beta^R(\beta_c^{(1)}) = 1/\pi \quad (22)$$

Thus plotting, e.g., the measured correlations $c^h(x)$ versus $-[c_4(x) + l^2 c_2^{(0)}(x)]$, we expect straight lines in the low-temperature phase. With increasing temperature, the slope should decrease until the critical slope $\mathcal{S}_c^{(1)} = 4/\pi \approx 1.273$ is reached at the transition. Typical results of such measurements are shown in Figure 10 for $l^2 = 3$ and $T = 3$. Since the measured slope ($\mathcal{S} \approx 1.33$) is only slightly larger than the critical, we can estimate $T_c^{(1)} \approx 3$.

At this transition, the fields A become effectively massive as a two-dimensional version of the Meissner effect in superconductivity (Kleinert, 1982*b*). As a consequence, the h correlations are screened at long range to [compare equation (8)]

$$c^h(x) = -4\beta^R l^2 c_2^{(0)}(x) \quad (23)$$

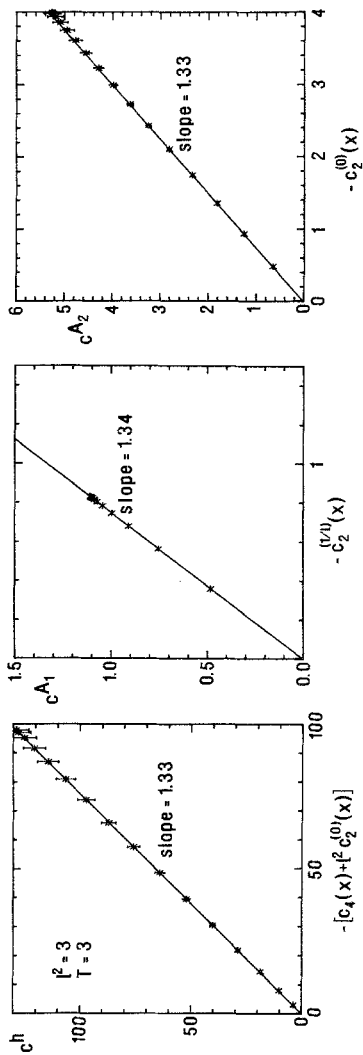


Fig. 10. Correlation functions of the two-dimensional second-gradient defect model for $l^2 = 3$ and $T = 3$ versus the theoretically expected behavior (20) in the low-temperature "solid" phase. The MC data are averages over 500,000 configurations.

which is exactly the behavior in the massless phase of the DG model. With further increasing temperature we expect therefore a second transition to a "liquid" phase (see footnote 3) where the h correlations also become massive. This happens for

$$\beta^R(\beta_c^{(2)}) = 1/2\pi l^2 \quad (24)$$

leading to a critical slope $\mathcal{F}_c^{(2)} = 2/\pi \approx 0.637$ in $c^h(x)$ versus $-c_2^{(0)}(x)$ plots similar to Figure 10. All transition points shown as open circles in the phase diagram in Figure 8 have been determined by this method.

5. CONCLUSION

Monte Carlo simulations of lattice defect models for melting based on the classical first-gradient energy exhibit in three dimensions a strong first-order transition, in agreement with theoretical analyses. Also in two dimensions we find a single first-order transition, which is, however, much weaker. This makes numerical analyses of this transition very difficult, as is well known from the experience with other models of statistical physics (e.g., exactly solvable Potts models).

Adding a second-gradient rotational energy, parametrized by the length scale l of rotational stiffness, yields a much richer model which can describe a variety of two-dimensional melting transitions. For small l , we still find a single first-order transition, but for increasing l , this separates into a sequence of two KT transitions. The generalized model should be relevant for explaining the systematics observed in recent experimental studies of the melting transition in adsorbed layers of long rodlike molecules (e.g., hydrocarbon chains). Certainly, while the structural simplicity of lattice defect models is best suited to uncover basic mechanisms, considerable refinements will be necessary to cope with realistic materials.

ACKNOWLEDGMENTS

I would like to thank Prof. D. Rogula for his kind invitation to this most interesting conference at Jablonna, and Prof. H. Kleinert for many stimulating discussions.

REFERENCES

- Ami, S., and Kleinert, H. (1984). *Journal de Physique*, **45**, L877.
 Banks, T., Myerson, R., and Kogut, J. (1977). *Nuclear Physics B*, **129**, 493.
 Berezinskii, V. L. (1970). *Zhurnal Eksperimental'noi i Teoreticheskoi Fizika*, **59**, 907 [*Soviet Physics—JETP* **32**, 493 (1971)].

- Berezinskii, V. L. (1971). *Zhurnal Eksperimental'noi i Teoreticheskoi Fizika*, **61**, 1144 [*Soviet Physics—JETP* **34**, 610 (1972)].
- Bowers, R. G., and Joyce, G. S. (1967). *Physical Review Letters*, **19**, 630.
- Bruce, D. A. (1985). *Materials Science Forum*, **4**, 51.
- Burton, J. A., Cabrera, N., and Frank, F. C. (1951). *Philosophical Transactions of the Royal Society of London A*, **243**, 299.
- Byckling, E. (1965). *Annals of Physics*, **32**, 367.
- Chui, S. T. (1982). *Physical Review Letters*, **48**, 933.
- Chui, S. T. (1983). *Physical Review B*, **28**, 178.
- Dasgupta, C., and Halperin, B. I. (1981). *Physical Review Letters*, **47**, 1556.
- Feynman, R. P. (1955). In *Progress in Low Temperature Physics*, Vol. 1, C. J. Gorter, ed., North-Holland, Amsterdam, p. 17.
- Gay, J. M., Suzanne, J., Pepe, G., and Meichel, T. (1988). *Surface Science*, **204**, 69.
- Gupte, N., and Shenoy, S. R. (1986). *Physical Review D*, **33**, 3002.
- Halperin, B. I., and Nelson, D. R. (1978). *Physical Review Letters*, **41**, 121 [Erratum, **41**, 519(E) (1978)].
- Helfrich, W. (1978). *Journal de Physique*, **39**, 1199.
- Jacobs, L., and Kleinert, H. (1984). *Journal of Physics A*, **17**, L361.
- Janke, W. (1985). Ph.D. thesis, FU Berlin (unpublished).
- Janke, W., and Kleinert, H. (1984). *Physics Letters*, **105A**, 143.
- Janke, W., and Kleinert, H. (1985). Unpublished results.
- Janke, W., and Kleinert, H. (1986a). *Nuclear Physics B*, **270**[FS 16], 135.
- Janke, W., and Kleinert, H. (1986b). *Physical Review B*, **33**, 6346.
- Janke, W., and Kleinert, H. (1986c). *Physics Letters*, **114A**, 255.
- Janke, W., and Kleinert, H. (1988). *Physical Review Letters*, **61**, 2344 [Erratum, **62**, 608(E) (1989)].
- Janke, W., and Kleinert, H. (1989). *Physics Letters*, **140A**, 513.
- Janke, W., and Kleinert, H. (1990). *Physical Review B*, **41**, 6848.
- Janke, W., and Toussaint, D. (1986). *Physics Letters*, **116A**, 387.
- Kapitza, P. L. (1937). *Nature* **141**, 74.
- Kapitza, P. L. (1941). *Journal of Experimental and Theoretical Physics (USSR)*, **11**, 1.
- Kleinert, H. (1982a). *Lettere Nuovo Cimento*, **34**, 103.
- Kleinert, H. (1982b). *Lettere Nuovo Cimento*, **34**, 464.
- Kleinert, H. (1982c). *Physics Letters*, **91A**, 295.
- Kleinert, H. (1982d). *Physics Letters*, **93A**, 86.
- Kleinert, H. (1983a). *Journal of Physics (Paris)*, **44**, 353.
- Kleinert, H. (1983b). *Physics Letters*, **95A**, 381.
- Kleinert, H. (1983c). *Physics Letters*, **95A**, 493.
- Kleinert, H. (1983d). *Lettere Nuovo Cimento*, **37**, 295.
- Kleinert, H. (1983e). *Physics Letters*, **96A**, 302.
- Kleinert, H. (1983f). *Physics Letters*, **97A**, 51.
- Kleinert, H. (1988a). *Physics Letters*, **130A**, 59.
- Kleinert, H. (1988b). *Physics Letters*, **130A**, 443.
- Kleinert, H. (1989a). *Gauge Fields in Condensed Matter*, World Scientific, Singapore.
- Kleinert, H. (1989b). *Physics Letters*, **136A**, 468.
- Kosterlitz, J. M. (1974). *Journal of Physics C*, **7**, 1046.
- Kosterlitz, J. M., and Thouless, D. J. (1973). *Journal of Physics C*, **6**, 1181.
- Kosterlitz, J. M., and Thouless, D. J. (1978). *Progress in Low Temperature Physics*, **7B**, 371.
- Larese, J. Z., Passell, L., Heidemann, A. D., Richter, D., and Wicksted, J. P. (1988). *Physical Review Letters*, **61**, 432.

- Lipa, J. A., and Chui, T. C. P. (1983). *Physical Review Letters*, **51**, 2291.
- Lund, F., Reisenegger, A., and Utreras, C. (1990). *Physical Review B*, **41**, 155.
- Minnhagen, P. (1987). *Review of Modern Physics*, **59**, 1001.
- Mueller, K. H., Ahlers, G., and Pobell, F. (1976). *Physical Review B*, **14**, 2096.
- Nelson, D. R. (1979). *Physical Review B*, **18**, 2318.
- Nelson, D. R. (1982). *Physical Review B*, **26**, 269.
- Nelson, D. R., and Halperin, B. I. (1979). *Physical Review B*, **19**, 2457.
- Nelson, D. R., and Toner, J. (1981). *Physical Review B*, **24**, 363.
- Nham, H. S., and Hess, G. B. (1988). *Physical Review B*, **38**, 5166.
- Onsager, L. (1949). *Nuovo Cimento Supplemento*, **6**, 249.
- Popov, V. N. (1973). *Zhurnal Eksperimental'noi i Teoreticheskoi Fizika* **64**, 672 [*Soviet Physics—JETP* **37**, 341 (1973)].
- Savit, R. (1980). *Review of Modern Physics*, **52**, 453.
- Shenoy, S. R. (1989). *Physical Review B*, **40**, 5056.
- Shockley, W. (1952). In *L'Etat Solide* (Proceedings of Neuvieme-Consail de Physique, Brussels), R. Stoops, ed., Institut de Physique, Solvay, Brussels.
- Shugard, W. J., Weeks, J. D., and Gilmer, G. H. (1978). *Physical Review Letters*, **41**, 1399 [Erratum, **41**, 1577(E) (1978)].
- Strandburg, K. J. (1986). *Physical Review B*, **34**, 3536.
- Strandburg, K. J. (1988). *Review of Modern Physics*, **60**, 161 (1988) [Erratum, **61**, 747(E) (1989)].
- Strandburg, K. J., Solla, S. A., and Chester, G. V. (1983). *Physical Review B*, **28**, 2717.
- Taub, H. (1988). In *The Time Domain in Surface and Structural Dynamics*, G. J. Long and F. Grandjean, eds., Kluwer, Dordrecht, p. 467.
- Ubbelohde, A. R. (1978). *The Molten State of Matter*, Wiley, New York.
- Vaks, V. G., and Larkin, A. I. (1965). *Zhurnal Eksperimental'noi i Teoreticheskoi Fizika*, **49**, 975 [*Soviet Physics—JETP*, **22**, 678 (1966)].
- Villain, J. (1975). *Journal de Physique*, **36**, 581.
- Wensley, R. J., and Stack, J. D. (1989). *Physical Review Letters*, **63**, 1764.
- Wiegel, F. W. (1973). *Physica*, **65**, 321.
- Wiegel, F. W. (1975). *Physics Reports*, **16**, 58.
- Wiegel, F. W. (1986). *Introduction to Path Integral Methods in Physics and Polymer Science*, World Scientific, Singapore.
- Williams, G. A. (1987). *Physical Review Letters*, **59**, 1926 [Erratum, **61**, 1142(E) (1988)].
- Young, A. P. (1979). *Physical Review B*, **19**, 1855.
- Zhang, S., and Migone, A. D. (1988). *Physical Review B*, **38**, 12039.
- Zhang, S., and Migone, A. D. (1989). *Surface Science*, **222**, 31.